Applied Geochemistry 100 (2019) 316–325

Contents lists available at ScienceDirect

Applied Geochemistry

journal homepage: www.elsevier.com/locate/apgeochem

# Determination of the available acid-generating potential of waste rock, part II: Waste management involvement

A. Elghali[a], M. Benzaazoua[a,*], B. Bussière[a], H. Bouzahzah[a,b]

[a] Université du Québec en Abitibi Témiscamingue, 445 Boul. Université, Rouyn-Noranda, QC, J9X 5E4, Canada
[b] Université de Liège, Génie minéral, matériaux et environnement, Allée de la découverte, 13/A. Bât. B52/3 Sart-Tilman, 4000, Liège, Belgique

ARTICLE INFO

Editorial handling by Dr. R. Seal

*Keywords:*
Waste rock
Waste rock sorting
Mineral liberation
Kinetic tests
Oxidation rate
Diameter of physical locking of sulfides

ABSTRACT

Open-pit mining operations often produce large amounts of waste rock that are characterized by large particle size distributions (PSD). Waste rock are normally deposited in surface piles that contain grains varying from a few microns to meters in size. Furthermore, the mineralogical and textural properties of the waste rock are influenced by their PSD. The diameter of physical locking of sulfides (DPLS) is a newly suggested parameter that was defined using an automated mineralogy system to separate waste rock according to their geochemical reactivity. Three lithologies (A, B, and C) were extracted from an open-pit gold mine and their geochemical behaviors, with respect to degree of sulfide liberation, were evaluated using column kinetic tests. The main results of this study showed that fine fractions of the studied waste rock were more sulfidic compared to coarse fractions. Moreover, sulfide liberation was negligible for fractions > 2.4 mm. Consequently, 2.4 mm was defined as the *critical diameter of sulfide reactivity* for the three studied waste rock. Column kinetic tests were used to confirm this hypothesis and to assess the geochemical behavior of the three lithologies. Geochemical analyses of leachates from the column tests showed that pH values remained between 7 and 8 and the instantaneous concentrations of metals such as iron (Fe) and zinc (Zn) were below environmental limits over the entire test duration (543 days). Considering sample reactivity, the data showed that the fine fractions primarily control the geochemical behavior of total samples. Sulfide oxidation rates were high for fractions < 2.4 mm, whereas they were negligible for fractions > 2.4 mm; total samples showed intermediate rates. For example, in lithology B, pyrite oxidation rates were 12.46 µmol/kg/day, 2.43 µmol/kg/day, and 0.27 µmol/kg/day for the fine fraction (< 2.4 mm), total sample (< 5 cm), and coarse fraction (> 2.4 mm) respectively. Sulfide and carbonate contents and their liberation were defined as key factors controlling the geochemical behavior of the studied waste rock, which was confirmed by the correlation factor between calcium leaching vs. carbonate liberation and between sulfur leaching vs. sulfide liberation. The coarse, unreactive fraction (> 2.4 mm) comprised a high proportion of the total sample weight (up to 90 wt. %). Screening waste rock, after blasting, according to the critical diameter of sulfide reactivity could be an efficient technique for global waste rock management that will reduce the economic costs related to waste rock pile reclamation.

## 1. Introduction

Over the last few decades, ore exploitation methods have evolved. Increasing metal prices and the availability of new equipment and technologies have allowed for the exploitation, usually by open-pit methods, of high-tonnage/low-grade ores. This type of exploitation generates large volumes of blasted and non-economic material called waste rock. Waste rock is part of the ore body that must be mined but is not treated because its metal content is lower than the operationally define cut-off grade. In general, waste rock is deposited in unsaturated piles that can be hundreds of meters in height and cover thousands of hectares (Aubertin et al., 2008; Bailey et al., 2016; Blowes et al., 2003). Interactions among atmospheric oxygen, water, and sulfide minerals (mainly pyrite and pyrrhotite) in the waste rock could lead to the release of metals/metalloids, sulfates, and acidity in drainage waters (Blowes et al., 1994; Bussière et al., 2005; Caldeira et al., 2003; Egiebor and Oni, 2007). In some cases, the neutralization potential of a waste rock is sufficient to neutralize the acidity produced by sulfide oxidation, but if the chemical quality of drainage waters does not respect the regulatory criteria it could cause environmental issues (Amos et al., 2015; Plante et al., 2011). Because of the way the material is deposited, waste rock piles are characterized by high chemical, physical,

* Corresponding author.
*E-mail address:* mostafa.benzaazoua@uqat.ca (M. Benzaazoua).

https://doi.org/10.1016/j.apgeochem.2018.12.010
Received 27 June 2018; Received in revised form 5 December 2018; Accepted 6 December 2018
Available online 08 December 2018
0883-2927/ 

mineralogical, and hydrogeological anisotropies (Aubertin et al., 2008; Bussière et al., 2011; Jamieson et al., 2015; Lefebvre et al., 2001; Smith et al., 2013). In general, waste rock piles are characterized by high heterogeneity of their internal structure, particularly regarding particle size distribution (PSD) (Poisson et al., 2009). These heterogeneities result from the methods used to construct the piles as well as particle segregation that could occur inside the piles due to water infiltration (McLemore et al., 2006). Generally, end- and push-dumping are the most used techniques for waste rock pile construction, both of which cause high internal structural heterogeneity in piles (Amos et al., 2015).

The environmental behavior of waste rock is controlled by their chemical, biological, mineralogical, and physical parameters (Aubertin et al., 2008; Blowes et al., 2003; Elghali et al., 2019; Jambor, 1994; Jamieson et al., 2015; Lindsay et al., 2009, 2015; Nordstrom, 2000, 2009; Nordstrom et al., 2015; Nordstrom and Southam, 1997; Paktunc, 1999a; Paktunc and Davé, 2000). Particle size is recognized as one of the most important factors controlling the reactivity of waste rock (Elghali et al., 2018; Erguler and Kalyoncu Erguler, 2015). Indeed, PSD determines waste rock reactivity by influencing the degree of liberation of acid-generating and neutralizing minerals (Elghali et al., 2018). The PSD of waste rock ranges from a few micrometers to meters in size (Bailey et al., 2016; Blowes et al., 2003, 2006) and will depend on the blasting technique and the type of lithology. The mineral exposure is correlated to the PSD and is defined as the degree of mineral liberation (Petruk and Lastra, 1993). This parameter is commonly used for mineral recovery during the flotation process and has been recently used as a key factor for environmental issues (Blowes et al., 2014; Brough et al., 2017; Erguler and Kalyoncu Erguler, 2015; Lapakko et al., 2006; Paktunc et al., 2000; Paktunc, 1999b; Parbhakar-Fox et al., 2017; Petruk et al., 1993). According to Elghali et al. (2018), waste rock could be separated into two fractions with highly different reactivities using automated mineralogical characterization. A new parameter, the diameter of physical locking of sulfides (DPLS), was defined that corresponds to the critical particle size where the degree of sulfide liberation becomes negligible (Elghali et al., 2018).

Three lithologies from an existing mine were sampled and characterized using a multi-disciplinary approach (Elghali et al., 2018). The main results of these characterizations showed that not all fractions are acid-generating, and at particle size bigger than 2.4 mm, the degree of sulfide liberation becomes negligible except for sulfides appearing at the surfaces of grains. This means that for coarse fractions (> 2.4 mm), negligible sulfide reactivity, and thus low acid production and metal release, could be expected. The main objectives of this companion paper are: i) to confirm that 2.4 mm is the DPLS, as is stated in Elghali et al. (2018), using column kinetic tests, and ii) to predict the long-term oxidation/neutralization potential of waste rock considering sulfide and carbonate mineral liberation.

## 2. Materials and methods

### 2.1. Field site and material preparation

The three studied lithologies were sampled in an open pit mine in Québec (Canada). The deposit constitutes a part of the Cadillac-Larder Lake tectonic zone (Helt et al., 2014). The deposit is an Archean gold porphyry consisting of ≤ 20 µm of disseminated gold (Helt et al., 2014). The mineralization is mainly related to altered clastic sediments such as greywacke, mudstone and some siltstone. The metasediments have undergone carbonate, silicic and potassic alteration. The three lithologies samples in this study were: carbonated porphyry (lithology A), altered greywacke (lithology B) and carbonated greywacke (lithology C).

The three lithologies were sampled from three sub-piles constructed in the field immediately after waste rock blasting. The three lithologies (A, B, and C) were homogenized using a quartering technique and a part of each lithology was sampled. The remaining samples were sieved with an aperture of 2.4 mm following the conclusions of the study by Elghali et al. (2018). Additional details about sampling, sample preparation, and characterizations can be found in Elghali et al. (2018). The particle diameter of 2.4 mm was defined as the DPLS for the three lithologies. Humid sieving was used to avoid fine particles attached at the surface of coarse particles (> 2.4 mm). At the end of this step, for each lithology, three samples were ready to be used in column leaching tests: i) samples with all grains < 5 cm, hereafter called *total sample;* ii) fractions between 5 cm and 2.4 mm, called *coarse fraction sample*; and iii) fractions < 2.4 mm, hereafter called *fine fraction sample*.

### 2.2. Methods

A total of nine columns was set up and run for 543 days: three columns for lithology A (total, fine, and coarse samples), three for lithology B (total, fine, and coarse samples), and three for lithology C (total, fine, and coarse samples). Columns were constructed from Plexiglas with a 28-cm inner diameter and 1-m height for the total samples and coarse fraction samples. For the fine fraction samples, a 14-cm inner diameter was used. Due to the PSD and column size, the masses of samples used in column tests were 64 kg for total samples and coarse fraction samples, and 10.25 kg for fine fraction samples. The columns with coarse and total samples were flushed monthly with 18 L of deionized water and columns with fine samples were flushed monthly with 2.7 L of deionized water. The water volume was chosen so as to keep the same liquid/solid ratio (L/S) for all columns. Samples were allowed to dry in ambient air between flushes. The leachates were collected and analyzed after 4 h of contact with samples.

At the end of the test, only columns with fine fractions were dismantled by collecting samples at depths of 1, 3, 5, 10, 15, 20, 25, and 38 cm. The solid samples were homogenized and analyzed for total sulfur and carbon content (wt.%) using an induction furnace (ELTRA CS-2000) with a detection limit of 0.009% and a precision of ± 5%. Soluble sulfates were analyzed using acid extraction with 40% HCl. Chemical composition for the first depth (1 cm) was analyzed using inductively coupled plasma atomic emission spectroscopy (ICP-AES). Samples collected at 1 cm depth were also analyzed using QEMSCAN® automated mineralogy to evaluate the degree of sulfide and carbonate liberation as well as probable sulfide coating. Solid chemical composition was analyzed by ICP-AES after the total digestion of samples using $HNO_3/Br_2/HF/HCl$. Some samples were analyzed using an aqua regia digestion, which yields a partial digestion of soluble minerals.

Leachate waters from the columns were analyzed for pH, Eh, electrical conductivity (EC), acidity, alkalinity, and chemical composition. The pH, Eh, and EC were analyzed using pH-Eh-conductivity meters. The acidity and alkalinity were analyzed using automated titration. The chemical composition of the leachates was analyzed using ICP-AES after sample acidification and filtration to 0.45 µm with 2% $HNO_3$. The soluble sulfates within the different leachates were analyzed using ionic chromatography with a precision of ± 5%. For each analysis, a blank is analyzed, and randomly selected samples were analyzed as duplicates. Results of duplicate analysis showed a reproducibility of more than 95%.

The mineralogy of initial samples and the 1-cm depth dismantled fine fractions was studied using Quantitative Evaluation of Minerals by Scanning Electron Microscopy (QEMSCAN®). QEMSCAN is an automated mineralogy system allowing detailed investigation of the mineralogical composition of samples mounted in polished sections. This system allows for the quantification of mineralogical parameters such as modal mineralogy, mineral liberation, and mineralogical association. Initial samples (≤ 5 mm) were sized by wet screening to produce five particle size fractions as described in Elghali et al. (2018). Several polished sections were analyzed by particle size fraction to produce enough data for good statistical representation. A total of more than 10000 grains were analyzed in fine fractions. The particle size fractions ≥ 5 mm were analyzed only using XRD. Furthermore, the computed

**Table 1**
ICP-AES and induction furnace chemical analyses of total, fine, and coarse fractions.

| | Detection limit (ppm) | Concentrations (%) | | | | | | | | | | | | |
|---|---|---|---|---|---|---|---|---|---|---|---|---|---|---|
| | | C | Al | Ba | Ca | Fe | K | Mg | Mn | Na | S | Si* | Ti | Zn (ppm) |
| | | 90 | 60 | 5 | 60 | 10 | 1 | 15 | 5 | 1 | 90 | – | 25 | 55 |
| Lithology A | Total sample (< 5 cm) | 0.51 | 8.13 | 0.11 | 2.05 | 2.56 | 2.3 | 0.82 | 0.03 | 3.33 | 0.24 | 30.4 | 0.17 | 60.18 |
| | Coarse fraction (> 2.4 mm) | 0.5 | 8.23 | 0.13 | 1.86 | 2.58 | 2.34 | 0.73 | 0.03 | 3.62 | 0.22 | 30.15 | 0.17 | 63.54 |
| | Fine fraction (< 2.4 mm) | 0.68 | 7.95 | 0.15 | 2.82 | 3.04 | 2.54 | 0.93 | 0.04 | 2.92 | 0.29 | 29.31 | 0.2 | 78.04 |
| Lithology B | Total sample (< 5 cm) | 0.26 | 8.3 | 0.06 | 2.27 | 4.41 | 2.17 | 1.81 | 0.05 | 2.78 | 0.48 | 29.4 | 0.32 | 84.06 |
| | Coarse fraction (> 2.4 mm) | 0.35 | 8.42 | 0.07 | 1.99 | 4.32 | 2.18 | 1.69 | 0.05 | 2.86 | 0.47 | 29.17 | 0.3 | 84.09 |
| | Fine fraction (< 2.4 mm) | 0.43 | 7.84 | 0.08 | 2.57 | 4.63 | 2.3 | 1.96 | 0.06 | 2.44 | 0.59 | 28.74 | 0.32 | 98.02 |
| Lithology C | Total sample (< 5 cm) | 0.29 | 8.32 | 0.06 | 2.04 | 4.12 | 2.33 | 1.63 | 0.05 | 2.6 | 0.49 | 28.98 | 0.3 | 78.01 |
| | Coarse fraction (> 2.4 mm) | 0.28 | 8.26 | 0.05 | 1.91 | 4.08 | 2.13 | 1.42 | 0.06 | 2.86 | 0.46 | 29.64 | 0.27 | 76.74 |
| | Fine fraction (< 2.4 mm) | 0.49 | 8.17 | 0.07 | 2.47 | 4.5 | 2.5 | 1.57 | 0.07 | 2.47 | 0.56 | 28.37 | 0.29 | 86.04 |

Si*: was analyzed using XRF whole rock analysis.

tomography was used to determine the sulfide liberation for fractions ≥5 mm (Elghali et al., 2018).

Samples post kinetic tests were sized by wet screening and Ro-Tap sieve shaking to produce two fractions: < 300 µm and > 300 µm to evaluate sulfide coating in these two fractions. This was used to identify if there was any preferential oxidation of sulfides dependent on the PSD. The polished sections for each fraction were analyzed by particle mineralogy analysis (PMA) mode. Measurement resolution varied from 2.5 µm to 6 µm depending on the particle size.

## 3. Results and discussion

### 3.1. Results

#### 3.1.1. Chemical and mineralogical characteristics of total, fine, and coarse fractions

*3.1.1.1. Chemical characterization.* Results of the chemical analyses of samples are summarized in Table 1. The chemical composition of studied samples is mainly composed by Si, Al, Fe, Na, Ca and K. Other elements such and C, S and Zn are marginally present. Silicon concentrations were > 28 wt. % for all nine samples (Table 1). Sulfur (totally as sulfide-sulfur) and carbon (totally as carbonate -carbon) concentrations were low compared to other elements. This is explained by the mineralogical composition of the tested lithologies which were mostly comprised of silicate minerals as is shown later. The only metals occurring in non-negligible concentrations within the samples were Fe, Al and Zn with concentrations around 2.5%, 8%, and 60 ppm, respectively. Additional details about the chemistry and distribution of elements can be found in Elghali et al. (2018).

*3.1.1.2. Mineralogical characteristics.* The mineralogical composition of the studied samples was determined using QEMSCAN (Elghali et al., 2018). Fig. 1 shows a summary of the mineralogical composition of the three lithologies. Sulfides consisted primarily of pyrite, as well as chalcopyrite, pyrrhotite, and sphalerite in trace amounts. Carbonate content was more significant within fine fractions (< 2.4 mm) for the three lithologies. Carbonates mainly occurred as calcite, but small concentrations of ankerite, dolomite, and rhodochrosite were found. The bulk mineralogical composition was dominated by non-sulfide gangue minerals, particularly quartz, albite, and muscovite.

Quantitatively, the 3 lithologies contained low sulfide contents (< 1 wt. %) and higher carbonate contents (> 2.2 wt. %). The sulfide minerals are enriched in fine to mid-size fraction (+53 µm/-300 µm) (Fig. 1). Carbonate contents decreased with the increase of the PSD. Sulfide contents were ~0.60 wt. %, 0.99 wt. %, and 1.04 wt. % for the lithologies A, B and C, respectively. Carbonate contents ranged from 3.2 wt. % to 5 wt. % for lithology A (Fig. 1), from 2.2 wt. % to 4.30 wt. % for lithology B (Fig. 1), and from 1.4 wt. % to 4.4 wt. % for lithology C (Fig. 1). Furthermore, quartz and albite contents were > 20 wt. % and > 10 wt. %, respectively, for all studied samples. Micas contents varied between 11 wt.% and 28 wt. % for lithology A, 15 wt. % and 32 wt. % for lithology B, and 23 wt. % and 35 wt. % for lithology C. Other identified minerals, with content lower than 5 wt. %, included: orthoclase, rutile, barite, apatite, Fe-oxide/Goethite and ankerite/dolomite.

*3.1.1.3. Calcium deportment.* The mineralogical composition of the studied samples shows Ca occurring in four minerals: calcite ($CaCO_3$), albite ($(Na,Ca)AlSi_3O_8$), and apatite ($Ca_5(PO_4)_3F$). Fig. 1S illustrates Ca deportment within the three waste rock lithologies. In lithology A (Fig. 1S–A), Ca mainly occurs within carbonates (calcite); about 64% for the total sample, 78% for the finer sample, and 71% for the coarse sample. In lithology B (Fig. 1S–B), only 36% of Ca comes from carbonates within the total sample, 51% for the finer sample, and 40% for the coarse sample. For lithology C (Fig. 1S–C), 44% of Ca is associated with carbonates in the total sample, 71% in the fine sample, and 45% in the coarse sample.

*3.1.1.4. Sulfur deportment.* Sulfur within the studied waste rock was associated with pyrite and barite. The two minerals differ in their involvement in mine drainage processes. Fig. 2S shows S deportment within the studied samples. For lithology A (Fig. 2S–A), 88% of S mainly occurs within pyrite in the total sample, 81% within the fine sample, and 80% within the coarse sample. For lithology B (Fig. 2S–B), approximately 97%, 93%, and 95% of S is associated with pyrite for the total, fine, and coarse samples, respectively. In lithology C (Fig. 2S–C), 97.5%, 98%, and 97.8% of S is associated with pyrite for the total, fine, and coarse samples, respectively.

*3.1.1.5. Mineral liberation degree.* In terms of mineral distributions/associations and textures, carbonates and sulfides within the studied lithologies displayed different degrees of liberation with respect to the particle size fractions (Fig. 2). The main conclusions drawn in the companion paper (Elghali et al., 2018) were that the sulfide liberation degree became negligible for particle sizes above 2.4 mm; however, carbonate liberation was higher than that of sulfides for the same particle size. Furthermore, static tests (acid base accounting and net acid generation tests) performed on the three lithologies showed that they could mostly be classified as non-acid-generating, although some fractions were classified as uncertain with respect to their acid generation potential. To confirm these static test predictions, column kinetic tests were performed.

#### 3.1.2. Kinetic leaching tests

Chemical results from the column kinetic tests (543 days) in terms of leachate quality are illustrated in Fig. 3, Fig. 4, and Fig. 5.

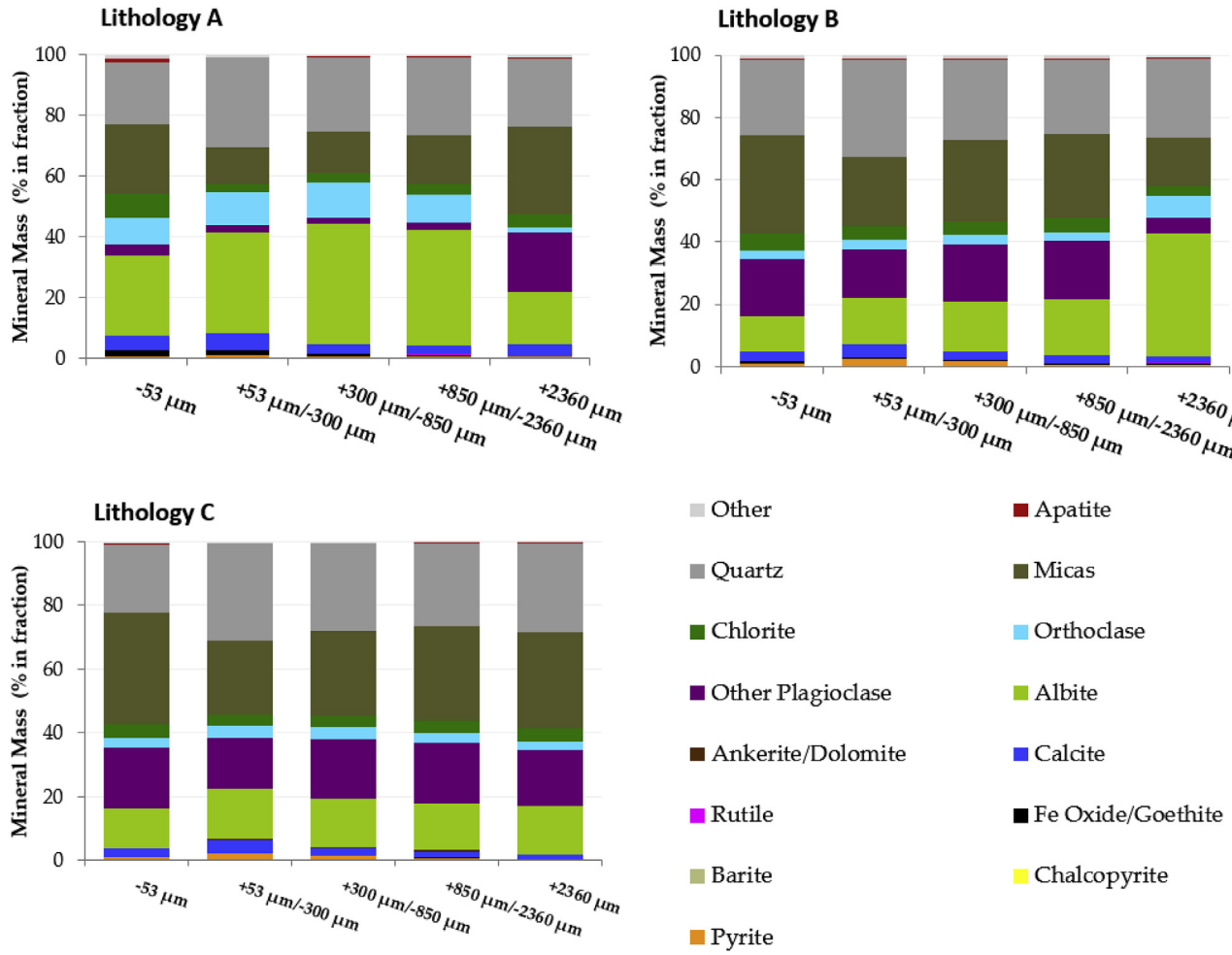


**Fig. 1.** Mineralogical composition of the three lithologies.

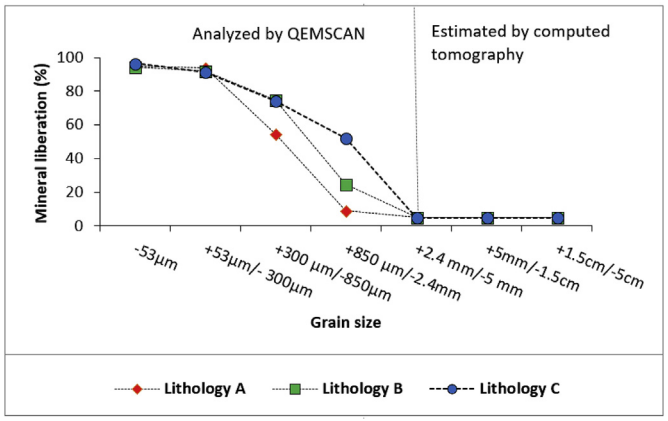


**Fig. 2.** Pyrite liberation degree within the three studied lithologies (adapted from Elghali et al., 2018).

Concentrations are presented as cumulative, mass-normalized releases (mg/kg) to allow for comparison of chemical release rates in the different samples (due to different sample weights in the column tests). Evolution of pH values (Fig. 3A) showed the same behavior for all nine samples, with circumneutral values (between 7.5 and 8.5). The three lithologies showed relatively similar pH during the kinetic tests. For each lithology, fine fraction samples showed lower pH values than total samples and coarse samples. Electric conductivity (Fig. 3B) varied considerably depending on sample particle size and lithology. The coarse samples showed the lowest EC values, while total samples showed medium values and fine samples showed the highest values. Average EC values were around 1000 µS/cm for fine samples, 60 µS/cm for coarse samples, and 220 µS/cm for total samples. Redox potential (Fig. 3C) was higher than 200 mV for all samples, suggesting oxidizing conditions. Alkalinity results (Fig. 3D) showed the same tendancy as EC; alkalinity was the highest for leachates from fine samples. The average alkalinity was smiliar for coarse and total samples at around 19 mg $CaCO_3$/L. However, for fine samples, the average alkalinity was variable depending on the lithology and equal to 49 mg $CaCO_3$/L for lithology A, 57 mg $CaCO_3$/L for lithology B, and 83 mg $CaCO_3$/L for lithology C.

Calcium, magnesium, and manganese were chosen to indicate neutralizing minerals dissolution (Benzaazoua et al., 2004), while silicon was assumed to be indicative of alumino-silicate mineral dissolution. Calcium, which occurs mainly as calcite, is the most leachable element as compared to Mg, Mn, and Si within the different samples, and Mn concentrations (occurring within ankerite) were the lowest. After 543 days of leaching tests, cumulative Ca charges were (Fig. 4A): 120 mg/kg for the total sample of lithology A, 66 mg/kg for the coarse fraction of lithology A, 238 mg/kg for the fine fraction of lithology A, 122 mg/kg for the total sample of lithology B, 33 mg/kg for the coarse fraction of lithology B, 529 mg/kg for the fine fraction of lithology B, 123 mg/kg for the total sample of lithology C, 37 mg/kg for the coarse fraction of lithology C and 461 mg/kg for the fine fraction of lithology C. Magnesium and manganese showed the same behavior as Ca, but at lower concentrations according to their initial concentrations in the solid samples. Silicon leaching was low compared to Ca leaching

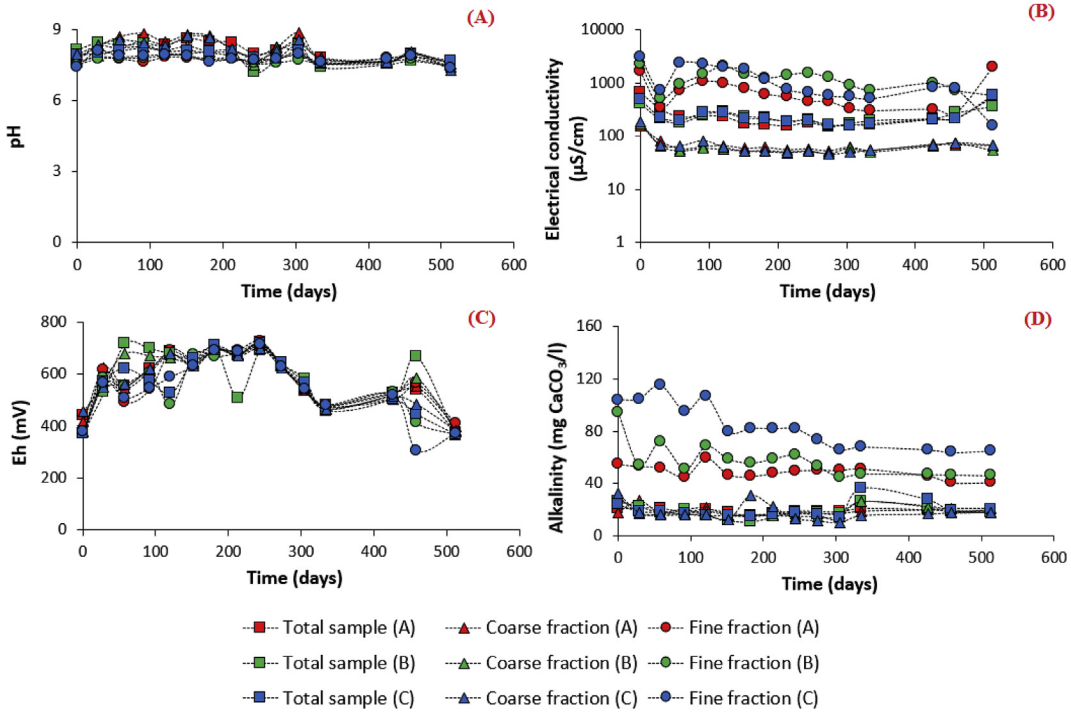


**Fig. 3.** Evolution of pH, EC, Eh and alkalinity within the different columns.

(Fig. 4D) in agreement with findings in the literature; Si leaching was less than 8.5 mg/kg for total samples and coarse fraction samples, and less than 23 mg/kg for fine fraction samples.

Sulfate, iron, and zinc leaching from the column tests is illustrated in Fig. 5. Sulfates, iron, and zinc (from sulfide oxidation) were leached in high concentrations from the fine samples relative to the coarse samples and total samples. After 543 days of leaching tests, total sulfates released (Fig. 5A) were about 262 mg/kg for the total sample of lithology A, 28 mg/kg for the coarse sample of lithology A, 493 mg/kg for the fine sample of lithology A, 2 mg/kg for the total sample of lithology B, 29 mg/kg for the coarse sample of lithology B, 1277 mg/kg for the fine sample of lithology B, 257 mg/kg for the total sample of lithology C, 32 mg/kg for the coarse sample of lithology C and 959 mg/kg for the fine sample of lithology C. Iron was leached in small concentrations (Fig. 5B). Iron was leached more in the fine samples (maximum of 0.16 mg/kg cumulative concentration). As expected, Zn

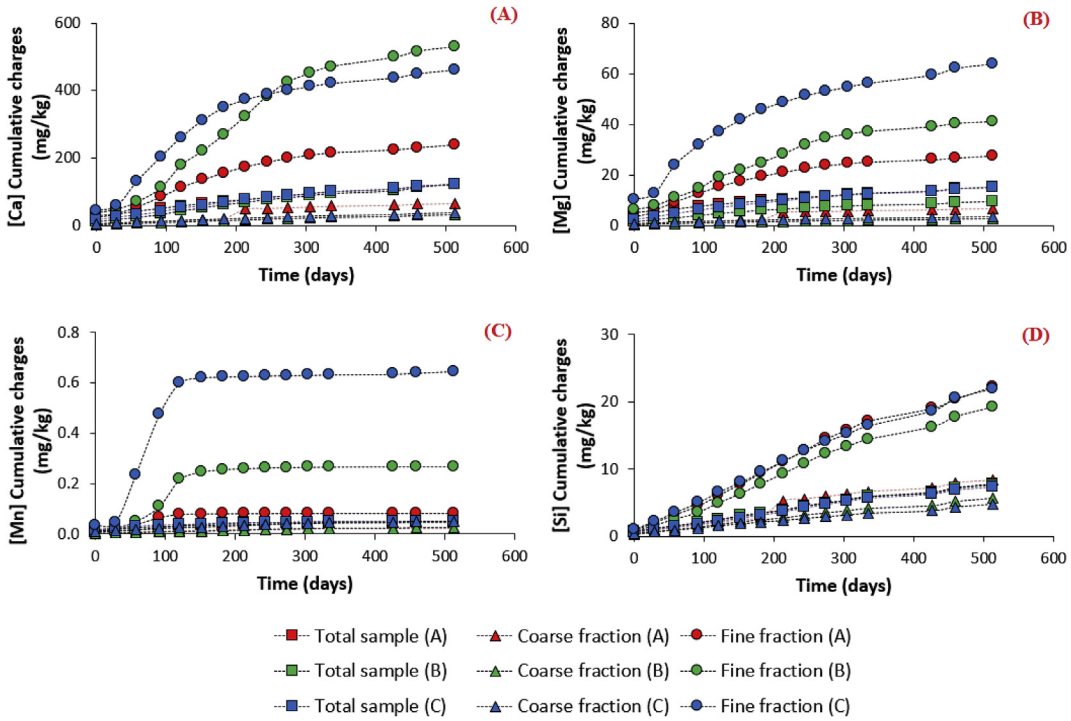


**Fig. 4.** Calcium, magnesium, manganese and silicon load in the studied samples. (For interpretation of the references to colour in this figure legend, the reader is referred to the Web version of this article.)

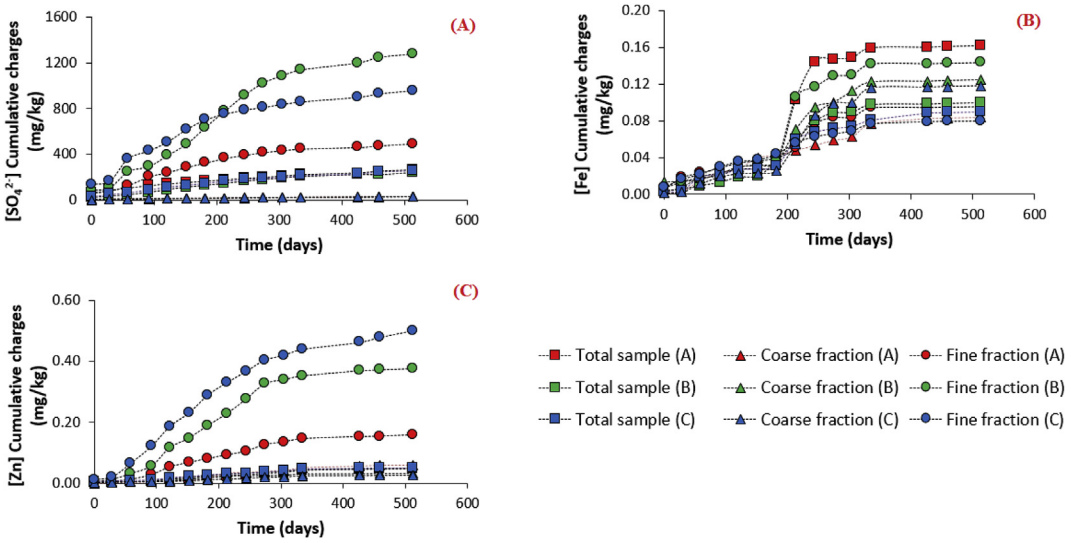


**Fig. 5.** Sulfates, iron, and zinc load within the studied samples.

was leached more in the fine samples (Fig. 5C); the maximum cumulative concentration was 0.5 mg/kg for the fine sample of lithology C.

### 3.1.3. Columns dismantlement results

Characterization of post-testing samples allowed for interpretation of the geochemical behavior and confirmation of assumptions. Only columns containing the fine samples for each lithology were dismantled and analyzed for total S, inorganic C, and sulfates. Results of the dismantlement are illustrated in Fig. 3S. The vertical profile of inorganic C concentrations showed a small variation between the top and bottom of the columns. Carbon concentrations ranged between 0.69% and 0.75% for lithology A, 0.40% and 0.44% for lithology B, and 0.46% and 0.50% for lithology C (Fig. 3S–A). The total S profiles (Fig. 3S–B) showed small variations. Total S concentrations ranged from 0.18 wt. % to 0.23 wt. % for lithology A, from 0.53 wt. % to 0.64 wt. % for lithology B, and from 0.49 wt. % to 0.56 wt. % for lithology C. Since initial sulfate concentrations within solid samples were below the limit of detection, sulfate analyses indicated sulfide oxidation and, more specifically, secondary mineral precipitation. The results of sulfate analyses for the three columns showed low concentrations, which indicate a low sulfide oxidation rate at the short time scale (cf Section 2). Sulfate concentrations were less than 0.023 wt. % for the three lithologies (Fig. 3S–C).

Automated mineralogical characterization was performed on dismantled samples to evaluate sulfide coating. Automated mineralogical characterization (QEMSCAN) of fine samples confirmed that carbonate and pyrite liberation degree depended on particle size (Fig. 6). In general, pyrite liberation was low within fractions > 300 µm, but carbonate liberation was higher for the same particle size. This means that there is more available neutralization potential than available acid generation potential within the three lithologies, which leads to the characterization of the long-term geochemical behavior of these lithologies as non-acid-generating. Furthermore, the alkalinity generated by fine fractions was greater than that generated by the total or coarse fraction samples during kinetic testing. Carbonates were less encapsulated (more reactive) when compared to sulfides for the coarse fractions (> 300 µm). Their encapsulation degrees (0–10% liberated) were about 52%, 26%, and 41% for lithologies A, B, and C, respectively. For fractions < 300 µm, carbonate encapsulation was about 2.50%, 4.40%, and 4.10% for lithologies A, B, and C, respectively. Sulfides were more encapsulated for fractions > 300 µm, and more liberated for fractions < 300 µm. For fractions > 300 µm, pyrite encapsulation was about 81%, 94%, and 77% for samples A, B, and C, respectively. However, for fractions < 300 µm, pyrite encapsulation was about 2.3%, 3.2%, and 0.8% for samples A, B, and C, respectively. Particle maps produced by QEMSCAN and backscattered-electron images showed that pyrite was encapsulated within non-sulfide gangue minerals for particle sizes > 300 µm. However, in fine fractions (< 300 µm), some pyrite grains were coated with a fine layer of iron oxides. The coating width was about 2–10 µm (Fig. 7) and pyrite had a particle size of about 20 − 60 µm. The proportion of coated pyrite was estimated to be between 5% and 22% depending on the lithology (using QEMSCAN data). This coating was not observed within the initial unweathered samples.

## 4. Discussion

Waste rock samples B and C could be considered to have similar lithologies, as they presented comparable mineralogical and chemical properties. Lithology A was slightly different in terms of sulfide and carbonate contents. In fact, lithology A was characterized by the highest carbonate content and the lowest sulfide content. These mineralogical and chemical differences influenced the geochemical responses in the kinetic tests performed on the three samples of each lithology. In general, these three lithologies are considered as non-acid-generating in the short-term since the leachate pH values were between 7 and 8 for the duration of the column tests. Additionally, concentrations of Fe and Zn (Fig. 8) collected immediately after each leaching cycle never exceeded environmental criteria (Directive 019 in Québec). With respect to the reactivity of these samples, the kinetic tests showed that the fine fractions of each lithology were the most reactive and mainly responsible for the overall geochemical behavior of the total sample. Table 2 summarizes the oxidation rates calculated for each sample over a period of 543 days. These results clearly show that the reactivity of the fine fractions is greater than that of the total samples and coarse fractions, regardless of the type of lithology. Based on the pyrite oxidation rates presented in Table 2, the fine fraction was two times more reactive than the total sample for lithology A, five times more reactive for lithology B, and four times more reactive for lithology C. This explains the high EC and alkalinity values observed within fine fractions as compared to total samples and coarse fractions for all of the lithologies.

Moreover, calculated pyrite oxidation rates for the nine studied samples were: 4.8 µmol/kg/day, 2.5 µmol/kg/day, and 0.3 µmol/kg/day for the fine, total, and coarse samples, respectively of lithology A; 12.5 µmol/kg/day, 2.4 µmol/kg/day, and 0.27 µmol/kg/day for the fine, total, and coarse samples, respectively of lithology B; and 9.4 µmol/kg/day, 2.5 µmol/kg/day, and 0.3 µmol/kg/day for the fine, total, and coarse samples, respectively of lithology C. These results confirmed the conclusions drawn from the study by Erguler and

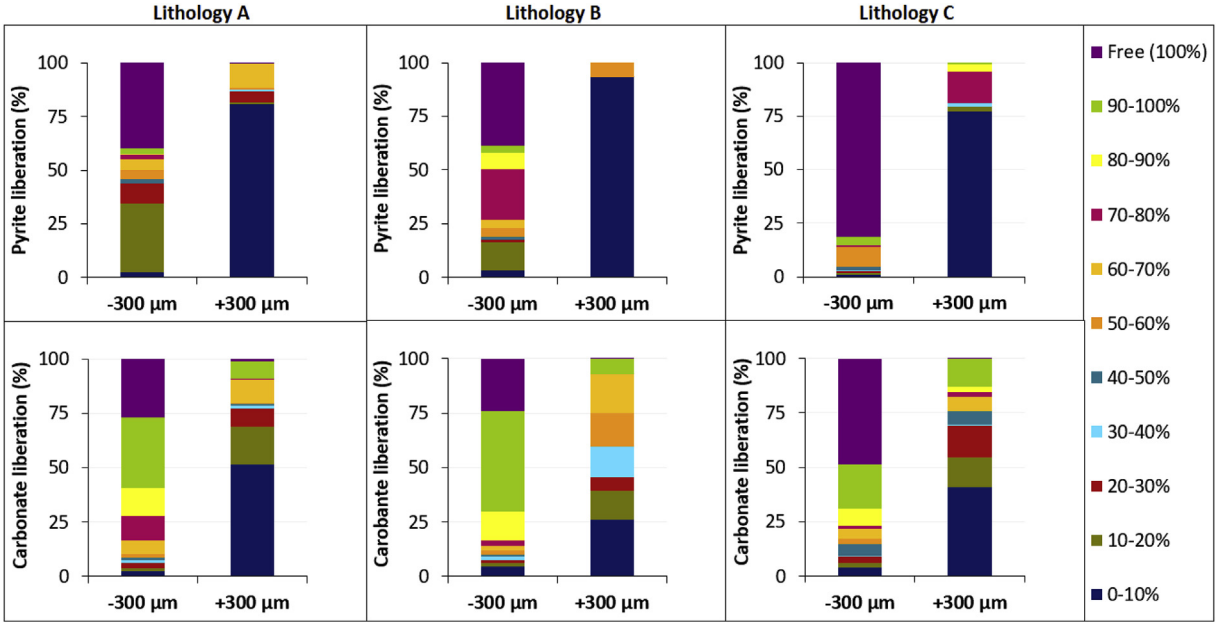


**Fig. 6.** Liberation degree of carbonate and pyrite in fine (< 2.4 mm) samples post-dismantlement.

Kalyoncu Erguler, 2015, who tested the overall effect of PSD on waste rock reactivity. Furthermore, calculated depletion times (Table 2) were approximately three times longer for carbonates than for sulfides.

Long-term predictions of geochemical behavior for the nine samples were performed using the oxidation/neutralization curves proposed by Benzaazoua et al. (2004), which use Ca + Mg + Mn releases as a tracer of neutralizing minerals dissolution, and sulphate releases as a tracer of sulfide oxidation. In this method, the initial concentrations in the solid

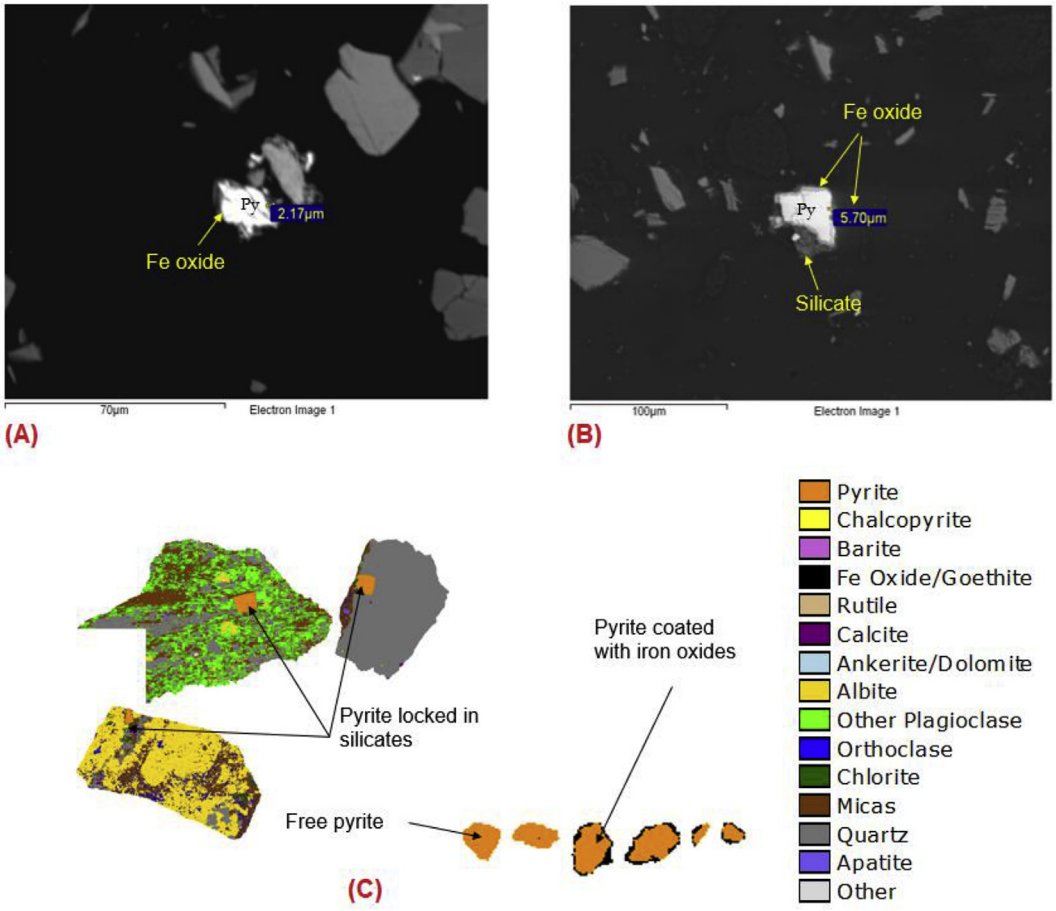


**Fig. 7.** A, B: backscattered-electron images for fine (< 2.4 mm) samples of lithology A; and C: false particle map showing an example of pyrite coating with iron oxides and free pyrite for lithology A.

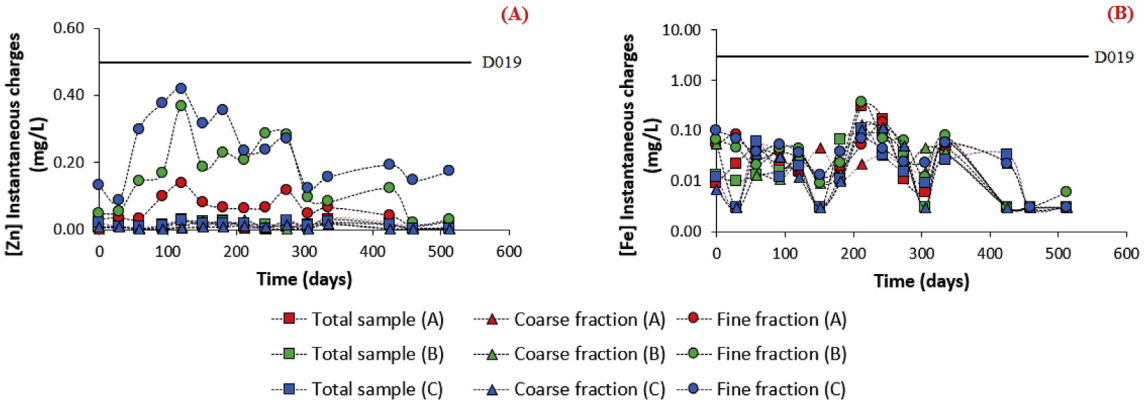


**Fig. 8.** Instantaneous Zn and Fe concentrations within the studied samples (D019 corresponds to directive 019 which is environmental standard used in Quebec (Canada) for mining projects).

samples are projected onto the graph Ca + Mg + Mn vs $SO_4^{2-}$ and the sample is classified as acid-generating if it is located on the side of sulphates and non-acid-generating if it is located on the side of Ca + Mg + Mn (Villeneuve et al., 2009). However, manganese was not used in this study as a neutralizing element because of its capacity to be hydrolyzed (Bouzahzah et al., 2015; Jambor et al., 2002; Lapakko, 1994). Therefore, only calcium and magnesium were used for the long-term prediction. Another issue related to the initial composition of solid samples consists of the use of total digestion analysis for projection. This assumes that the reactive minerals (sulfides and carbonates) will react completely on a long-term scale. However, only soluble minerals and exposed parts of the sulfides and carbonates will be able to react. In this study, two ways are suggested to solve this issue: i) use results of an aqua regia digestion, which gives a partial digestion of solid samples, and/or ii) correction of the total digestion results with mineral liberation data. Oxidation/neutralization curves for the nine samples are shown in Fig. 4S. The three types of projections (total digestion, aqua regia digestion, and chemistry corrected by mineral liberation) showed that the different studied samples are classified as non-acid-generating regardless of the type of projection used. This is explained by the high NP of the studied samples compared to their AP.

Since the three fine fraction samples of each lithology are characterized by a different liberation degree of sulfides and carbonates, Ca and S leaching rates were different for each sample. Calcium and sulfur concentrations were normalized to the initial mass of Ca and S for each sample to avoid the effect of initial chemical/mineralogical differences. Calcium and sulfur concentrations were recorded over the kinetic test period and plotted against the liberation degree of carbonates and sulfides, respectively. The linear regressions for both elements are displayed in Fig. 9 and show a high correlation coefficient between S leaching and pyrite liberation degree on one side and between Ca leaching and carbonate liberation degree on the other side. Indeed, the correlation coefficient between S leaching and sulfide liberation was 0.95; the correlation coefficient between Ca leaching and carbonate liberation was 0.93. These results confirm and complement previous conclusions of other studies which demonstrated that sample particle size greatly influences reactivity (Amos et al., 2015; Brough et al., 2017; Erguler and Kalyoncu Erguler, 2015; Lapakko et al., 2006; Smith et al., 2000), but in this study, the quantitative aspect of the effect of mineral liberation on the geochemical behavior of mine waste rock is highlighted as an important factor controlling mineral reactivity.

## 5. Methodological guide for waste rock characterization

Considering these results, which confirm the conclusions of Elghali et al. (2018), a new method for waste rock management is suggested in which waste rock could be separated into two fractions with extremely different reactivities. This could be accomplished by defining the DPLS of a waste rock, which is a critical particle size that delimits the reactive fraction of a given sulfide-bearing waste rock (Elghali et al., 2018). For this parameter, fractions smaller than the DPLS are largely responsible for the reactivity of the total sample, while the larger fraction has a minimal effect. Therefore, this parameter could be used to separate waste rock prior to the construction of conventional waste rock piles. This technique could considerably reduce the costs associated with waste rock pile reclamation and management in cases where the waste rock contains a higher sulfur content.

The proposed methodology for waste rock management is illustrated in Fig. 10. This proposed methodology consists of sampling materials in the field (< 5 cm) after blasting operations to consider the particle size distribution. The collected samples should be separated into several fractions; then submitted to chemical assays and static tests to evaluate the acid-generating potential of these fractions. Acid base accounting and net acid generation tests are two of the most used tests for these purposes. Next, the fine fractions (< 5 mm) should be characterized using an automated mineralogy system, while the coarse

**Table 2**
Results of sulfide oxidation rate, oxidation/neutralization curves and S/Ca depletion.

| Lithology | Sample | Sulfide oxidation rate (μmol/kg/day) | Oxidation/neutralization curves | | Sulfur depletion curves | | | Calcium depletion curves | | |
|---|---|---|---|---|---|---|---|---|---|---|
| | | | $R^2$ | Slope | $R^2$ | Slope | Depletion (year) | $R^2$ | Slope | Depletion (year) |
| A | < 2.4 mm | **4.84** | 0.998 | 0.55 | 0.88 | -1E-04 | 2739 | 0.89 | -2E-05 | 13698 |
| | < 5 cm | 2.50 | 0.999 | 0.56 | 0.96 | -5E-05 | 5479 | 0.97 | -9E-06 | 30441 |
| | > 2.4 mm | 0.26 | 0.913 | 3.26 | 0.97 | -3E-06 | 91324 | 0.87 | -7E-06 | 39139 |
| B | < 2.4 mm | **12.46** | 0.996 | 0.445 | 0.92 | -1E-04 | 2740 | 0.93 | -4E-05 | 6849 |
| | < 5 cm | 2.43 | 0.977 | 0.539 | 0.96 | -3E-05 | 9132 | 0.98 | -1E-05 | 27397 |
| | > 2.4 mm | 0.27 | 0.995 | 1.298 | 0.96 | -3E-06 | 91324 | 0.99 | -3E-06 | 91324 |
| C | < 2.4 mm | **9.41** | 0.993 | 0.585 | 0.85 | -9E-05 | 3044 | 0.81 | -3E-05 | 9132 |
| | < 5 cm | 2.45 | 0.999 | 0.530 | 0.96 | -3E-05 | 9132 | 0.97 | -1E-05 | 27397 |
| | > 2.4 mm | 0.30 | 0.988 | 1.120 | 0.96 | -4E-07 | 684932 | 0.99 | -3E-07 | 913242 |

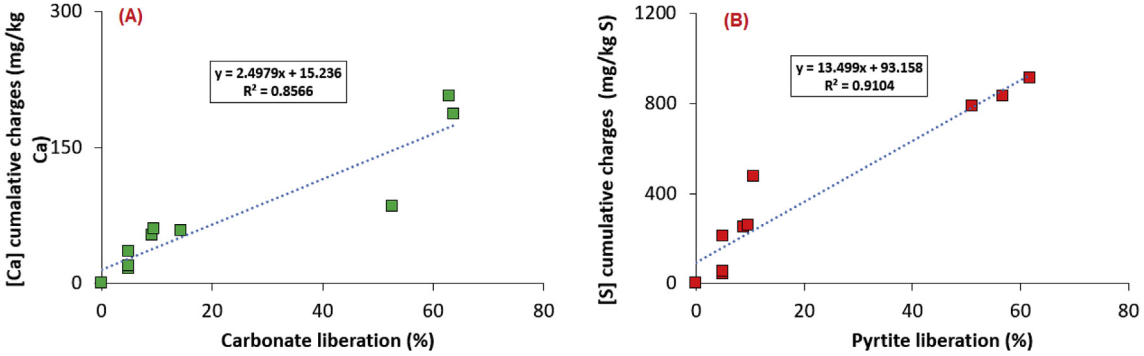


**Fig. 9.** Projection of Ca leached vs carbonate liberation (A) and S leached vs. pyrite liberation (B).

fractions (> 5 mm) should be characterized using computed tomography to evaluate sulfide liberation. Subsequently, the DPLS can be defined (Elghali et al., 2018). Using this diameter and based on the results of static tests, kinetic tests could be performed to evaluate the reactivity of samples under the defined DPLS, above the defined DPLS, and for the total sample. Thus, the results from automated mineralogical analyses and computed tomography could be confirmed.

## 6. Conclusion

The main objectives of this study were to confirm that 2.4 mm is the diameter of physical locking of sulfides within the three studied lithologies and to evaluate the geochemical behavior of these lithologies through kinetic testing. The results showed that fine fractions are the most sulfidic and where mineral liberation is higher relative to coarser fractions. The three studied lithologies showed similar geochemical behaviors. Within the three studied samples, carbonate contents were higher than sulfide contents, which explains the neutral

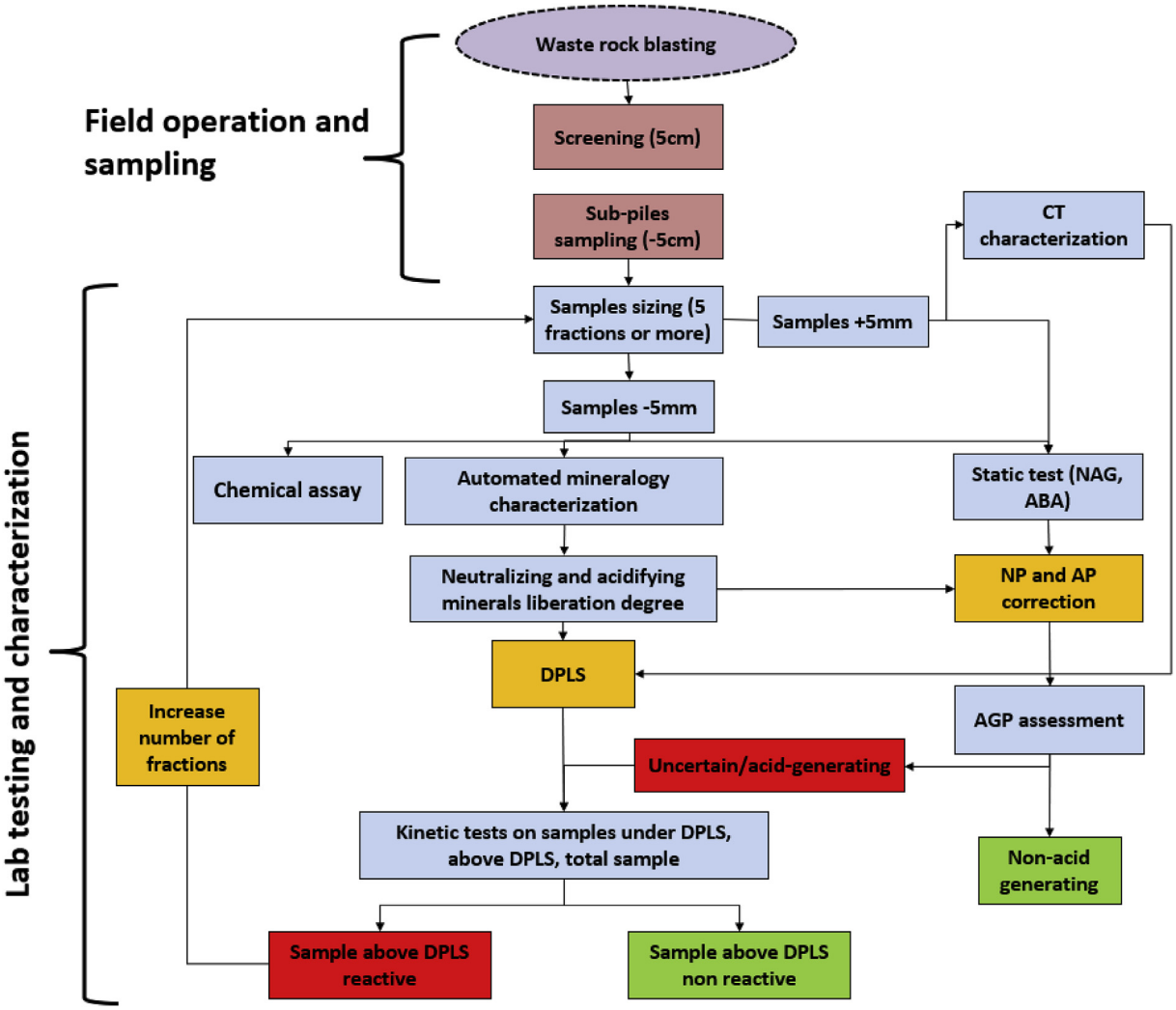


**Fig. 10.** Proposed methodology for waste rock characterization for environmental purposes.

behavior observed during the 534-day kinetic test. However, sulfide oxidation rates and species release rates were completely different depending on the sample (< 2.4 mm, > 2.4 mm, < 5 cm). The sulfide oxidation rate was higher for lithologies B and C than for lithology A due to their initial sulfide contents. Sulfide content was significant within lithologies B and C, which are considered to have the same petrogenesis (greywackes).

With respect to the effect of particle size distribution, fine fractions (< 2.4 mm) showed high oxidation rates compared to coarse fractions (> 2.4 mm) and to total samples (< 5 cm) due to different degrees of sulfide mineral liberation. Fine fractions were characterized by high sulfide mineral liberation compared to total samples. The samples containing only fractions > 2.4 mm showed very low oxidation rates and low species release rates due to their low sulfide mineral liberation. Linear regressions of sulphate releases vs sulfide mineral liberation and Ca release vs carbonate mineral liberation showed correlation coefficients; about 0.95 for sulphates and 0.93 for calcium. The two equations established for mineral liberation (sulfides and carbonates) and species release (Ca and S) could be used as a tool for predicting species leaching for samples with known carbonate and sulfide mineral liberation.

## Acknowledgements

The authors thank URSTM staff for their support with materials testing and analysis. Funding of this study was provided by the NSERC UQAT industrial research chair in Mine site reclamation and its partners (Canadian Malartic mine, Glencore Raglan mine, Rio-Tinto Fe-Ti, Agnico-Eagle mines, IAMGold).

## Appendix A. Supplementary data

Supplementary data to this article can be found online at https://doi.org/10.1016/j.apgeochem.2018.12.010.

## References

Amos, R.T., Blowes, D.W., Bailey, B.L., Sego, D.C., Smith, L., Ritchie, A.I.M., 2015. Waste-rock hydrogeology and geochemistry. Appl. Geochem. 57, 140–156.

Aubertin, M., Fala, O., Molson, J., Chouteau, M., Anterrieu, O., Hernandez, M.A., Chapuis, R.P., Bussière, B., Lahmira, B., Lefebvre, R., 2008. Caractérisation du comportement hydrogéologique et géochimique des haldes à stériles. In: Paper presented at the Proceedings: Symposium.

Bailey, B.L., Blowes, D.W., Smith, L., Sego, D.C., 2016. The Diavik Waste Rock Project: Geochemical and microbiological characterization of low sulfide content large-scale waste rock test piles. Appl. Geochem. 65, 54–72. https://doi.org/10.1016/j.apgeochem.2015.10.010.

Benzaazoua, M., Bussière, B., Dagenais, A.-M., Archambault, M., 2004. Kinetic tests comparison and interpretation for prediction of the Joutel tailings acid generation potential. Environ. Geol. 46 (8), 1086–1101. https://doi.org/10.1007/s00254-004-1113-1.

Blowes, D., Ptacek, C., Jambor, J., Weisener, C., 2003. The geochemistry of acid mine drainage. Treatise Geochem. 9, 612.

Blowes, D., Ptacek, C., Jambor, J., Weisener, C., Paktunc, D., Gould, W., Johnson, D., 2014. The geochemistry of acid mine drainage.

Blowes, D., Moncur, M., Smith, L., Sego, D., Bennet, J., Garvie, A., Linklater, C., Gould, D., Reinson, J., 2006. Construction of two large-scale waste rock piles in a continuous permafrost region. In: Paper presented at the Proceedings-7th International Conference on Acid Rock Drainage (ICARD), St Louis. Mo. US.

Blowes, D.W., Jambor, J.L., Alpers, C.N., 1994. The environmental geochemistry of sulfide mine-wastes, vol 22 Mineralogical Association of Canada.

Bouzahzah, H., Benzaazoua, M., Plante, B., Bussiere, B., 2015. A quantitative approach for the estimation of the "fizz rating" parameter in the acid-base accounting tests: A new adaptations of the Sobek test. J. Geochem. Explor. 153, 53–65. https://doi.org/10.1016/j.gexplo.2015.03.003.

Brough, C., Strongman, J., Bowell, R., Warrender, R., Prestia, A., Barnes, A., Fletcher, J., 2017. Automated environmental mineralogy; the use of liberation analysis in humidity cell testwork. Miner. Eng. 107, 112–122.

Bussière, B., Aubertin, M., Zagury, G.J., Potvin, R., Benzaazoua, M., 2005. Principaux défis et pistes de solution pour la restauration des aires d'entreposage de rejets miniers abandonnées. In: Paper presented at the Symposium 2005 sur l'environnement et les mines.

Bussière, B., Demers, I., Dawood, I., Plante, B., Aubertin, M., Peregoedova, A., Pepin, G., Lessard, G., Intissar, R., Benzaazoua, M., 2011. Comportement géochimique et hydrogéologique des stériles de la mine Lac Tio. In: Paper presented at the Proceedings of the Symposium sur l'Environnement et les Mines. Rouyn-Noranda, CD-Rom, CIM, Montreal.

Caldeira, C.L., Ciminelli, V.S.T., Dias, A., Osseo-Asare, K., 2003. Pyrite oxidation in alkaline solutions: nature of the product layer. Int. J. Miner. Process. 72 (1–4), 373–386. https://doi.org/10.1016/S0301-7516(03)00112-1.

Egiebor, N.O., Oni, B., 2007. Acid rock drainage formation and treatment: a review. Asia Pac. J. Chem. Eng. 2 (1), 47–62.

Elghali, A., Benzaazoua, M., Bouzahzah, H., Bussière, B., Villarraga-Gómez, H., 2018. Determination of the available acid-generating potential of waste rock, part I: Mineralogical approach. Appl. Geochem. 99, 31–41. https://doi.org/10.1016/j.apgeochem.2018.10.021.

Elghali, A., Benzaazoua, M., Bussière, B., Kennedy, C., Parwani, R., Graham, S., 2019. The role of hardpan formation on the reactivity of sulfidic mine tailings: A case study at Joutel mine (Québec). Sci. Total Environ. 654, 118–128. https://doi.org/10.1016/j.scitotenv.2018.11.066.

Erguler, Z.A., Kalyoncu Erguler, G., 2015. The effect of particle size on acid mine drainage generation: Kinetic column tests. Miner. Eng. 76, 154–167. https://doi.org/10.1016/j.mineng.2014.10.002.

Helt, K.M., Williams-Jones, A.E., Clark, J.R., Wing, B.A., Wares, R.P., 2014. Constraints on the genesis of the Archean oxidized, intrusion-related Canadian Malartic gold deposit, Quebec, Canada. Econ. Geol. 109 (3), 713–735.

Jambor, J., 1994. Mineralogy of sulfide-rich tailings and their oxidation products. Environ. Geochem. Sulfide Mine-Waste. 22, 59–102.

Jambor, J., Dutrizac, J., Groat, L., Raudsepp, M., 2002. Static tests of neutralization potentials of silicate and aluminosilicate minerals. Environ. Geol. 43 (1–2), 1–17.

Jamieson, H.E., Walker, S.R., Parsons, M.B., 2015. Mineralogical characterization of mine waste. Appl. Geochem. 57, 85–105. https://doi.org/10.1016/j.apgeochem.2014.12.014.

Lapakko, K.A., 1994. Evaluation of neutralization potential determinations for metal mine waste and a proposed alternative. In: Paper presented at the Proceeding: of the Third International Conference on the Abatement of Acidic Drainage, April.

Lapakko, K.A., Engstrom, J.N., Antonson, D.A., 2006. Effects of particle size on drainage quality from three lithologies. In: Paper presented at the Poster paper presented at the 7th International Conference on Acid Rock Drainage (ICARD).

Lefebvre, R., Hockley, D., Smolensky, J., Gélinas, P., 2001. Multiphase transfer processes in waste rock piles producing acid mine drainage: 1: Conceptual model and system characterization. J. Contam. Hydrol. 52 (1–4), 137–164. https://doi.org/10.1016/S0169-7722(01)00156-5.

Lindsay, M.B.J., Condon, P.D., Jambor, J.L., Lear, K.G., Blowes, D.W., Ptacek, C.J., 2009. Mineralogical, geochemical, and microbial investigation of a sulfide-rich tailings deposit characterized by neutral drainage. Appl. Geochem. 24 (12), 2212–2221. https://doi.org/10.1016/j.apgeochem.2009.09.012.

Lindsay, M.B.J., Moncur, M.C., Bain, J.G., Jambor, J.L., Ptacek, C.J., Blowes, D.W., 2015. Geochemical and mineralogical aspects of sulfide mine tailings. Appl. Geochem. 57, 157–177. https://doi.org/10.1016/j.apgeochem.2015.01.009.

McLemore, V.T., Donahue, K.M., Phillips, E., Dunbar, N., Walsh, P., Gutierrez, L.A., Tachie-Menson, S., Shannon, H.R., Lueth, V.W., Campbell, A.R., 2006. *Characterization of Goathill North Mine Rock Pile, Questa Molybdenum Mine, Questa, New Mexico.* Paper presented at the International Conference of Acid Rock Drainage (ICARD). ASMR, St. Louis.

Nordstrom, D.K., 2000. Advances in the hydrogeochemistry and microbiology of acid mine waters. Int. Geol. Rev. 42 (6), 499–515.

Nordstrom, D.K., 2009. Acid rock drainage and climate change. J. Geochem. Explor. 100 (2–3), 97–104. https://doi.org/10.1016/j.gexplo.2008.08.002.

Nordstrom, D.K., Southam, G., 1997. Geomicrobiology of sulfide mineral oxidation. Rev. Mineral. 35, 361–390.

Nordstrom, D.K., Blowes, D.W., Ptacek, C.J., 2015. Hydrogeochemistry and microbiology of mine drainage: An update. Appl. Geochem. 57, 3–16.

Paktunc, A., 1999a. Mineralogical constraints on the determination of neutralization potential and prediction of acid mine drainage. Environ. Geol. 39 (2), 103–112.

Paktunc, A., Davé, N., 2000. Mineralogy of pyritic waste rock leached by column experiments and prediction of acid mine drainage. In: Rammlmair, D. (Ed.), Applied Mineralogy, pp. 621–623 Paper presented at the, Balkema.

Paktunc, A.D., 1999b. Characterization of mine wastes for prediction of acid mine drainage *Environmental impacts of mining activities*. Springer, pp. 19–40.

Parbhakar-Fox, A., Lottermoser, B., Hartner, R., Berry, R.F., Noble, T.L., 2017. Prediction of Acid Rock Drainage from Automated Mineralogy *Environmental Indicators in Metal Mining*. Springer, pp. 139–156.

Petruk, W., Lastra, R., 1993. Evaluation of the recovery of liberated and unliberated chalcopyrite by flotation columns in a copper cleaner circuit. Int. J. Miner. Process. 40 (1), 137–149. https://doi.org/10.1016/0301-7516(93)90046-D.

Poisson, J., Chouteau, M., Aubertin, M., Campos, D., 2009. Geophysical experiments to image the shallow internal structure and the moisture distribution of a mine waste rock pile. J. Appl. Geophys. 67 (2), 179–192.

Smith, K.S., Ramsey, C.A., Hageman, P.L., 2000. Sampling strategy for the rapid screening of mine-waste dumps on abandoned mine lands. US Department of the Interior, US Geological Survey.

Smith, L.J., Bailey, B.L., Blowes, D.W., Jambor, J.L., Smith, L., Sego, D.C., 2013. The Diavik Waste Rock Project: Initial geochemical response from a low sulfide waste rock pile. Appl. Geochem. 36, 210–221.

Villeneuve, M., Bussière, B., Benzaazoua, M., Aubertin, M., 2009. Assessment of interpretation methods for kinetic tests performed on tailings having a low acid generating potential. Proceedings, Securing the Future and 8th ICARD, Skelleftea, Sweden.